European Coordination for Accelerator Research and Development

PUBLICATION

CAVITY BEAM POSITION MONITOR SYSTEM FOR ATF2

Boogert, S T (John Adams Institute at Royal Holloway University of London) *et al*

01 December 2011

The research leading to these results has received funding from the European Commission under the FP7 Research Infrastructures project EuCARD, grant agreement no. 227579.

This work is part of EuCARD Work Package **9: Technology for normal conducting higher energy linear accelerators**.

The electronic version of this EuCARD Publication is available via the EuCARD web site <http://cern.ch/eucard> or on the CERN Document Server at the following URL : <http://cdsweb.cern.ch/record/1403148

CAVITY BEAM POSITION MONITOR SYSTEM FOR ATF2*

S. T. Boogert†, G. Boorman, F. Cullinan, N. Joshi, A. Lyapin, JAI at Royal Holloway, Egham, UK
A. Aryshev, Y. Honda, T. Naito, N. Terunuma, J. Urakawa, KEK, Tsukuba, Japan
A. Heo, E-S Kim, Y.I. Kim, KNU, Daegu, Korea
D. McCormick, J. Frisch, J. Nelson, T. Smith, G. R. White, SLAC, Menlo Park, CA, USA

Abstract

The Accelerator Test Facility 2 (ATF2) in KEK, Japan, is a prototype scaled demonstrator system for the final focus required for a future high energy lepton linear collider. The ATF2 beam-line is instrumented with a total of 41 high resolution C and S band resonant cavity beam position monitors (BPM) with associated mixer electronics and digitisers. In addition 4 high resolution BPMs have been recently installed at the interaction point, we briefly describe the first operational experience of these cavities in the ATF2 beam-line. The current status of the overall BPM system is also described, with a focus on operational techniques and performance.

INTRODUCTION

The ATF2 is a scaled demonstrator for Raymondi-Seryi final focus systems which are planned for future linear colliders (LC). The aim of the ATF2 is two fold, firstly to obtain and verify a vertical focus size of 37 nm, secondly to hold the focus stable to within a few nanometres. To achieve these challenging goals at ATF2 there are a total of 41 position sensitive dipole cavities: 35 normal C-band cavities for the extraction, matching and final focus sections, 4 S-band used in the final focusing doublet (where a larger aperture is required due to the large beam size there) and 2 interaction point (IP) cavities (IPBPMs). The C and S-band BPMs are rigidly located in a quadrupole, the first 10 BPMs are mounted in fixed quadrupoles, whilst the next 27 are mounted in quadrupoles which are moved by three axis mover magnet movers and the 4 IP region BPMs (2 normal C-band and 2 IPBPMs) are rigidly fixed, but not in magnets. The interaction point IPBPMs are required to monitor the beam orbit at the interaction point beam size monitor and also a proxy measurement of beam size as beam jitter should scale linearly with beam size.

Cavities

The cavities used at ATF2 are cylindrical or rectangular cavities which are coupled via rectangular slots into waveguides ending with coaxial adaptors. This arrangement allows to extract the position sensitive dipole cavity mode and suppress the strong monopole modes. The BPMs have 4 symmetric couplers, two for each transverse plane.

* The research leading to these results has received funding from the European Commission under the FP7 Research Infrastructures project EuCARD, grant agreement no.227579.

† stewart.boogert@rhul.ac.uk

A cavity output $\tilde{V}_{\rm cavity}$ is an exponentially decaying sine wave, with frequency ω and decay constant τ, where subscript of d denotes dipole and r reference. For the dipole output $\tilde{V}_d$, the amplitude and phase depends on the bunch charge q, length σ_z, position x, angles θ and tilt α and arrival time of the bunch, and the decay time defined by the coupling strength and internal losses.

$$\tilde{V}_{\rm d} = \left[A_x x + jA_\theta\theta - jA_\alpha\alpha\right] qe^{-t/\tau_d} e^{j(\omega_d t+\phi_d)} \quad (1)$$

Additional reference cavities, operating at the same frequencies as the position cavities for C-band and at the image frequency for S-band, provide an independent combined measurement of the bunch charge, length and arrival time, so that these can be used in the position determination. So the reference output $\tilde{V}_r$ is

$$\tilde{V}_r = A_q q e^{-t/\tau_r} e^{j(\omega_r t+\phi_r)} \quad (2)$$

Furthermore, the voltage produced due to angle and tilt is in quadrature phase with respect to the position signal, and can be separated from it using the reference cavity phase, thus only leaving the position dependence in the signal.

Signal Processing and Calibration

The electronics are single-stage image rejection mixers. Most of the C-band CBPM output signals are attenuated by 20 dB to avoid saturation of the digitiser system and simplify the digital processing algorithm. The phase of the local oscillator (LO) signal for the C-band electronics is locked to the accelerator low level radio frequency (RF) system, while the S-band LO is free running. The intermediate frequency (IF) is around 20-30 MHz for both C and S-band. Down-converted signals are digitised at 100 MHz by 14-bit digitisers.

$$\tilde{V}_{\rm elec} = \tilde{G}\tilde{V}_{\rm cavity} = Ge^{j\phi_{\rm elec}}\tilde{V}_{\rm cavity}, \quad (3)$$

where $\tilde{G}_{cavity}$ is electronics complex gain. The VME processor-controller hosting the digitisers publishes the waveform data through EPICS. The entire processing system is also readout via EPICS and controlled via Python scripting language. The digital signal processing described below is performed in a dedicated data-driven C program, that monitors the arrival of beam, computes the relevant parameters and publishes the resulting output via EPICS. The state of the CBPM system is viewed via a simple EDM application that can view both the raw and processed data.The digitised IF signals from the electronics are then demodulated digitally using a complex LO signal and filtered to

remove the up-converted component and out of band noise. The resulting complex envelope is sampled at roughly one filter length after the amplitude peak at time t_s and normalised by the reading produced by the reference channel.

$$I + jQ = \frac{\tilde{V}_{\rm d}(t = t_{s,d}, \omega_d = 0)}{\tilde{V}_{\rm r}(t = t_{s,r}, \omega_r = 0)} \quad (4)$$

This phasor $I + jQ$ is then rotated by an angle θ_{IQ}, so $I' + jQ' = e^{i\theta_{IQ}}(I + iQ)$ in such a way that its real, or in-phase I' component is proportional to the position and the imaginary, or quadrature Q' component only contains the angle and tilt information. The required rotation of the IQ plane is measured during the calibration when there is significant position variation compared with angular. The calibration consists of 2 stages. Firstly, the digital LO frequency is tuned for each channel by minimising the gradient of the phase of the down-converted signal. The position scale for converting I' into position S and the IQ rotation are measured by either moving the quadrupole which holds the BPM or by performing a 4-magnet closed orbit bump for the cavities which are rigidly fixed.

Interaction Point Region BPMs

The IPBPMs also operate at C-band but there are some significant differences. An IPBPM block, consisting of two dipole cavities fabricated together, shown in Fig. 1 was installed at the end of 2010 to understand the beam orbit around the focus of the ATF2. The main operational difference between this BPM and the other C-band BPMs is the x direction resonant frequency is 5.7086 GHz and the decay time of the signal is significantly shorter. A separate x-frequency reference cavity was also installed approximately 10 m from the interaction point. The four vertical dipole signals are processed in the electronics developed for normal C-band BPMs and using the same local oscillator as the other C-band cavity BPMs at ATF2. The x dipole and reference signals are mixed using a separate LO. A test installation of two IPBPM blocks is installed at an upstream location [4] for high resolution performance studies using two stage homodyne downmix electronics [5]. In addition to the two IPBPM cavities, two normal C-band BPMs have been commissioned either side of the interaction point, so called pre and post IP BPMs. A downconverted signal from an IPBPM is shown in Fig. 2.

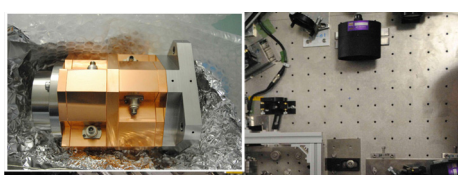

Figure 1: Large : IP location of ATF2, insert : IPBPM block before installation.

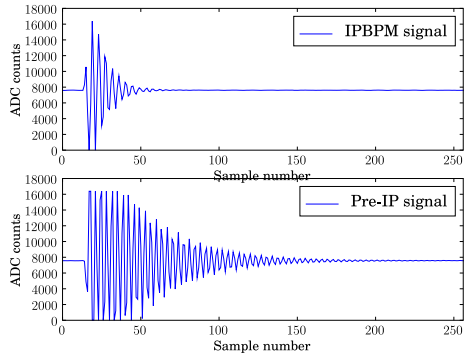

Figure 2: Example of raw digitised downconverted signals, from (top) an IPBPM, compared with (bottom) a normal C-band BPM (Pre-IP).

System Performance

The entire BPM system has been operating well since 2009. All 41 BPMs were calibrated and a model independent analysis used to compute the resolution of each BPM [1] using 500 ATF extractions. Figure 3 shows a summary of all the BPM resolutions. The BPMs with attenuators have consistent resolution in both x and y directions of 250 nm. A study of the best achievable resolution, using the unattenuated four sequential BPMs, yielded a best resolution of 27 nm for a bunch charge of $\sim 0.3 \times 10^{10}$ e/bunch. The IP region BPMs did not have consistent measured resolution, but the best performing IPBPM achieved a resolution of $\sim$ 150 nm, an order of magnitude larger than previously obtained of 8.7 nm using these cavities [5]. This is not surprising as the beam alignment through 4 fixed lo-

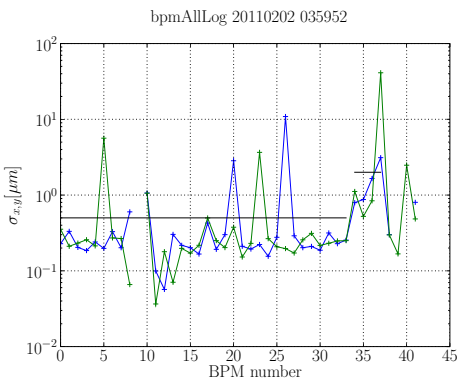

Figure 3: BPM resolution as a function of BPM index along the ATF2 beamline. The horizontal lines are a cut used to determine which BPMs have poor resolution. C-band BPMs are labelled 1-33, unattenuated C-band are 11-14, S-band are 34-37, Pre-IP is 38, IPBPMs are 39-40 and Post-IP is 41.

cation cavities is extremely challenging and the signal processing algorithm has not yet been optimised for the shorter decay time. A detailed study of the best achievable resolution is ongoing at ATF2 at an upstream location [4].

SYSTEM STABILITY

The overall system stability is essential for continuous high performance operation. Table 1 shows constants for repeated calibrations for a single BPM, which show clear scale variations of 10%. Over longer timescales, the variation of calibration constants has been significantly larger up to 50% in scale and a full rotation in phase [1, 2]. The

Table 1: Calibration Constants Calculated from five Consecutive Calibrations in x with and without Jitter Subtraction

Run	With jitter		Jitter subtracted	
	Scale	IQ rotation	Scale	IQ rotation
1	-89.44	-0.0108	-100.15	-0.0130
2	-108.79	-0.0138	-99.44	-0.0151
3	-99.80	-0.0203	-100.83	-0.0189
4	-90.16	-0.0233	-101.09	-0.0249
5	-103.30	-0.0378	-101.26	-0.0243

signal processing electronics are monitored by a test tone injection system. The electronics vary by at most 1% in gain and 1° in phase over long time scales, so another effect was causing the variation in BPM calibration constants. A

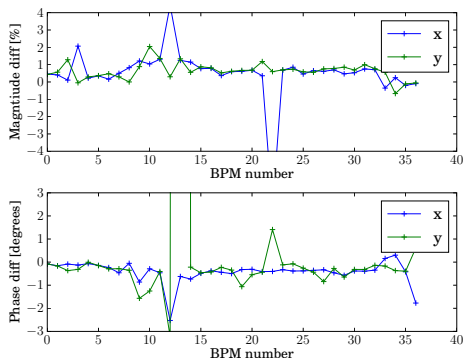

Figure 4: Electronics relative gain G_d/G_r and phase $\phi_{elec,d} - \phi_{elec,r}$ compared at two different times separated by 4 days. The figure only shows 37 BPMs as the IP region BPMs did not have test tones.

detailed study on the scale stability was performed [2]. We find that jitter dominates the scale uncertainty and if monitored and removed the calibration scale measurements are more stable.

The observed variation of the phase angle of the position sensitive signal can not be explained only by beam jitter variation. From Eqns. 1 and 2 the ratio of dipole to reference responses is

$$\frac{\tilde{V}_d}{\tilde{V}_r} = \frac{A_d}{A_r} e^{-\Delta\Gamma(t_s - t_0)} e^{j\Delta\omega(t_s - t_0)} . \quad (5)$$

where $\Delta\omega$ and $\Delta\Gamma$ is the difference between dipole and reference cavity frequencies and decay constants respectively and t_0 is the time at which the digitiser starts. The variation in digitiser start was measured by fitting a straight line to the rising edge diode rectified reference cavity signal. At bunch charges of 0.3×10^{10} electrons per bunch t_0 varied as much as 0.5 ns, whilst at 0.8×10^{10} the fluctuation has reduced to 30 ps. From Eqn. 5 variation in digitiser start or sample time would change the normalised signal phase by $\Delta\omega\Delta t$. Any variation in the dipole frequency relative to reference $\Delta\omega$ will also cause variations in θ_{IQ}. Different temperatures or temperature dependence of a dipole-reference pair will cause a frequency shift, so a phase rotation of the I-Q phasor. The frequency temperature dependence of a normal C-band cavity is of order 100 kHz/K, so assuming a maximum temperature variations of 1 K, and $t_s - t_0$ of 300 ns results in phase shift of 11° at C-band, compared with the 1° achieved by the electronics. It is possible to monitor the relative dipole-reference phase or cavity frequencies using beam data but this requires relatively large signals in the dipole cavity to make an accurate determination. As the beam orbit and charge dictate the cavity signal amplitudes, a passive method of measuring the temperature of the cavity and correcting for frequency changes is adopted. Each BPM has been recently instrumented with a copper-constantin thermistor with a readout resolution of 0.1°C.

CONCLUSIONS AND OUTLOOK

The ATF2 cavity BPM system is operating well with measured resolutions approaching what is required for the ILC. From recent studies at the ATF and via simulations it appears that scale S variations are mainly driven by beam jitter and not electronics gain variation. The calibration rotation θ_{IQ} variation is more dependent on trigger start variations and thermally induced cavity frequency shifts. A temperature system was installed, with the aim of removing the thermal effect and rotation corrections based on a diode beam arrival detector have been implemented. These effects need to be studied in further detail during the Autumn of 2011 before the system is considered stable and hence fully commissioned. New IPBPMs have been installed and operated but need further work to realise their full resolution potential at the IP. Finally, studies are ongoing to establish if this system will operate with an International Linear Collider like bunch spacings of between 150 and 300 ns.

REFERENCES

[1] S. T. Boogert *et al*, IPAC'10, Kyoto, Japan, August 2010, MOPE070

[2] F. Cullinan *et al*, these proceedings, TUPC025

[3] N. Joshi *et al*, these proceedigns, TUPC164

[4] Y. I. Kim *et al*, these proceedings, TUPC119

[5] Y. Inoue *et al.*, PRSTAB 11, 062801, (2008)